NANO LETTERS
Letter
Cite This: Nano Lett. 2017, 17, 7951−7961
pubs.acs.org/NanoLett

# A Nanobionic Light-Emitting Plant

Seon-Yeong Kwak,[†] Juan Pablo Giraldo,[†,‡] Min Hao Wong,[†] Volodymyr B. Koman,[†] Tedrick Thomas Salim Lew,[†] Jon Ell,[†] Mark C. Weidman,[†] Rosalie M. Sinclair,[†] Markita P. Landry,[§] William A. Tisdale,[†] and Michael S. Strano*[,†]

[†]Department of Chemical Engineering, Massachusetts Institute of Technology, 77 Massachusetts Aveue, Cambridge, Massachusetts United States

[‡]Department of Botany and Plant Sciences, University of California, 3401 Watkins Drive, Riverside, California United States

[§]Department of Chemical and Biomolecular Engineering, University of California, 201 Gilman Hall, Berkeley, California United States

Supporting Information

**ABSTRACT:** The engineering of living plants for visible light emission and sustainable illumination is compelling because plants possess independent energy generation and storage mechanisms and autonomous self-repair. Herein, we demonstrate a plant nanobionic approach that enables exceptional luminosity and lifetime utilizing four chemically interacting nanoparticles, including firefly luciferase conjugated silica (SNP-Luc), D-luciferin releasing poly(lactic-*co*-glycolic acid) (PLGA-$LH_2$), coenzyme A functionalized chitosan (CS-CoA) and semiconductor nanocrystal phosphors for longer wavelength modulation. An in vitro kinetic model incorporating the release rates of the nanoparticles is developed to maximize the chemiluminescent lifetimes to exceed 21.5 h. In watercress (*Nasturtium officinale*) and other species, the nanoparticles circumvent limitations such as luciferin toxicity above 400 $\mu$M and colocalization of enzymatic reactions near high adenosine triphosphate (ATP) production. Pressurized bath infusion of nanoparticles (PBIN) is introduced to deliver a mixture of nanoparticles to the entire living plant, well described using a nanofluidic mathematical model. We rationally design nanoparticle size and charge to control localization within distinct tissues compartments with 10 nm nanoparticles localizing within the leaf mesophyll and stomata guard cells, and those larger than 100 nm segregated in the leaf mesophyll. The results are mature watercress plants that emit greater than $1.44 \times 10^{12}$ photons/sec or 50% of 1 $\mu$W commercial luminescent diodes and modulate "off" and "on" states by chemical addition of dehydroluciferin and coenzyme A, respectively. We show that CdSe nanocrystals can shift the chemiluminescent emission to 760 nm enabling near-infrared (nIR) signaling. These results advance the viability of nanobionic plants as self-powered photonics, direct and indirect light sources.

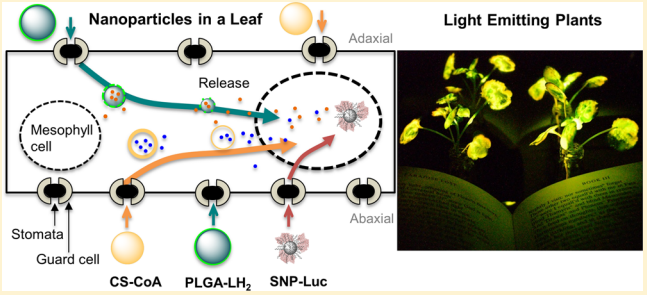


**KEYWORDS:** *Plant nanobionics, nanoparticles, pressurized bath infusion of nanoparticles (PBIN), light-emitting plant, chemiluminescence*

As independent energy sources, plants are adapted for persistence and self-repair in harsh environments.[1] They are therefore compelling platforms for engineering new functions, such as light emission and information transfer. Attempts to generate light-emitting plants have previously focused on genetic engineering using either the firefly luciferase gene[2] or bacterial *lux* operon.[3] A central complication with this approach is the difficulty in colocalizing reactive enzymes for chemiluminescence within substrate producing regions and high adenosine triphosphate (ATP) concentration,[4] requiring external administration of 1 mM luciferin in the case of the former, despite its toxicity to plant cells above 400 $\mu$M.[2] Recent advances from our laboratory in the engineering of nanoparticle have enabled their trafficking and localization in specific organelles within living plants,[1,5−7] offering new opportunities to control the location and concentrations of light-generating reactions within living, wild-type plants. In this work, we develop a plant nanobionic approach that utilizes the size and surface charges of four distinct nanoparticle types to control their distribution in and around the plant mesophyll, generating light-emitting variants of several common wild-type plants such as spinach (*Spinacia oleracea*), arugula (*Eruca sativa*), watercress (*Nasturtium officinale*), and kale (*Brassica oleracea*), which were selected because of their empirically observed high ATP production rates.

The firefly luciferase−luciferin reaction pathway is a commonly employed system utilizing ATP within an organism

Received: October 12, 2017
Revised: November 13, 2017
Published: November 17, 2017





DOI: 10.1021/acs.nanolett.7b04369
Nano Lett. 2017, 17, 7951−7961

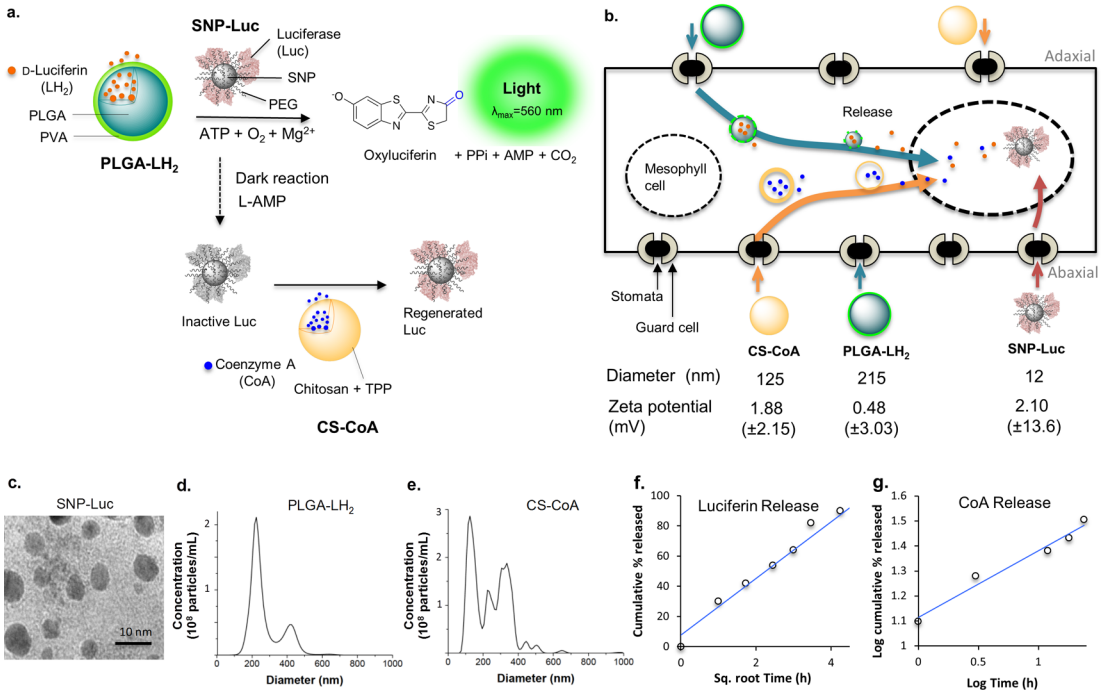


**Figure 1.** Preparation of nanoparticle system for light production. (a) Reaction mechanism of light production by firefly luciferase using nanoparticles. In the presence of adenosine triphosphate (ATP), oxygen ($O_2$), and magnesium ions ($Mg^{2+}$), the firefly luciferase (Luc; pink lumps) immobilized silica nanoparticles (SNP-Luc; gray sphere) catalyze the oxidation of luciferin ($LH_2$; orange dots) that is released from luciferin-loaded PLGA nanoparticles (PLGA-$LH_2$; blue-green sphere) encapsulated by a poly(vinyl alcohol) (PVA) layer (yellow-green). Dehydroluciferyl-adenylate (L-AMP) is formed as a byproduct, acting as a strong inhibitor of the luciferase. Coenzyme A (CoA; blue dots) released from CoA-encapsulated chitosan nanoparticles (CS-CoA; apricot sphere) opposes this inhibitory effect of L-AMP by triggering the thiolytic reaction, which regenerates luciferase activity. (b) Schematic illustration of nanoparticles in a leaf. SNP-Luc, PLGA-$LH_2$, and CS-CoA are separately prepared and infiltrated into the plant as a mixture to enter the leaf tissues through the stomatal pores on the abaxial and adaxial sides. The smaller SNP-Luc can enter the stomatal guard cells and the mesophyll cells, wherease the larger PLGA-$LH_2$ and CS-CoA stay in the mesophyll and release $LH_2$ (orange dots) and CoA (blue dots) as the polymer nanoparticles are swollen and biodegraded. The released $LH_2$ and CoA can then enter the cytosol, where ATP exists in high concentration. Diameters and zeta potential of the nanoparticles are shown below the illustration. (c) Transmission electron microscopy image of SNP-Luc. Concentration and size distribution of (d) PLGA-$LH_2$ and (e) CS-CoA. Releasing kinetics of (f) PLGA-$LH_2$ and (g) CS-CoA nanoparticles for 24 h at room temperature.

to generate yellow-green photoemission, centered at 560 nm, via the oxidation of D-luciferin ($LH_2$) catalyzed by firefly luciferase in the presence of ATP, $Mg^{2+}$, and $O_2$ (Figure 1a).[8−10]

$$LH_2 + ATP + O_2 \xrightarrow[Mg^{2+}]{\text{Luciferase}} \text{Oxyluciferin} + AMP + PPi + CO_2 + h\nu\ (\text{Light}) \quad (1)$$

Three different chemically interacting nanoparticles with controlled size and surface charge are rationally designed and fabricated to target specific compartments of the leaf (Figure 1b). Firefly luciferase (a monomeric 61 kDa) was immobilized onto maleimide-functionalized 7 nm silica nanoparticles (SNP-Luc, Figure 1c), which are expected to increase the stability of the enzyme[11] within a living plant and help the intact enzyme efficiently traverse the plant cell membrane as per our recently developed mechanism.[6] To overcome luciferin toxicity in plant cells, poly(lactic-*co*-glycolic acid) (PLGA) nanoparticle (Figure 1d,f) was synthesized to supply a high extracellular flux of luciferin while suppressing the local concentration. Chitosan-tripolyphosphate (CS) carriers were used to release coenzyme A (CoA) (Figure 1e,g) because CoA extends the light emission by regenerating firefly luciferase activity via a reaction with dehydroluciferyl-adenylate, a strong inhibitor of light production ($IC_{50}$ = 5 nM).[12,13]

$$\text{Luciferase-L-AMP} \xrightarrow{\text{CoA}} \text{Luciferase} + \text{L-CoA} + AMP \quad (2)$$

The 10−15 $\mu$m stomatal pores on the both adaxial and abaxial sides of a leaf are highly permeable to nanoparticles,[14] but once in the mesophyll nanoparticle size and surface charge can be utilized to direct and restrict specific localization as we have shown in recent work[6] (Figure 1b). SNP-Luc is designed to enter leaf mesophyll cells and stomata guard cells and localize near the organelles, chloroplasts, and mitochondria, where ATP generation is highest.[15] The larger PLGA-$LH_2$ and CS-CoA are intended to remain within the leaf mesophyll intercellular spaces as releasing the reagents to be subsequently transported through the cell walls and membranes.

We studied the chemical interactions (1) and (2) that result when PLGA-$LH_2$, CS-CoA, and SNP-Luc are combined with 0.5 mM ATP to optimize the release kinetics and nanoparticle concentrations for light emission and duration. While SNP-Luc exhibits 36% lower turnover number than free luciferase, illumination is more than doubled (Figure 2a). The addition of PLGA-$LH_2$ and CS-CoA over direct addition of $LH_2$ and CoA extends the light duration by 3.2 times longer (Figure 2a). There is a notable trade-off between initial reaction rate and overall duration. For example, 4 $\mu$M SNP-Luc generates a


DOI: 10.1021/acs.nanolett.7b04369
Nano Lett. 2017, 17, 7951−7961

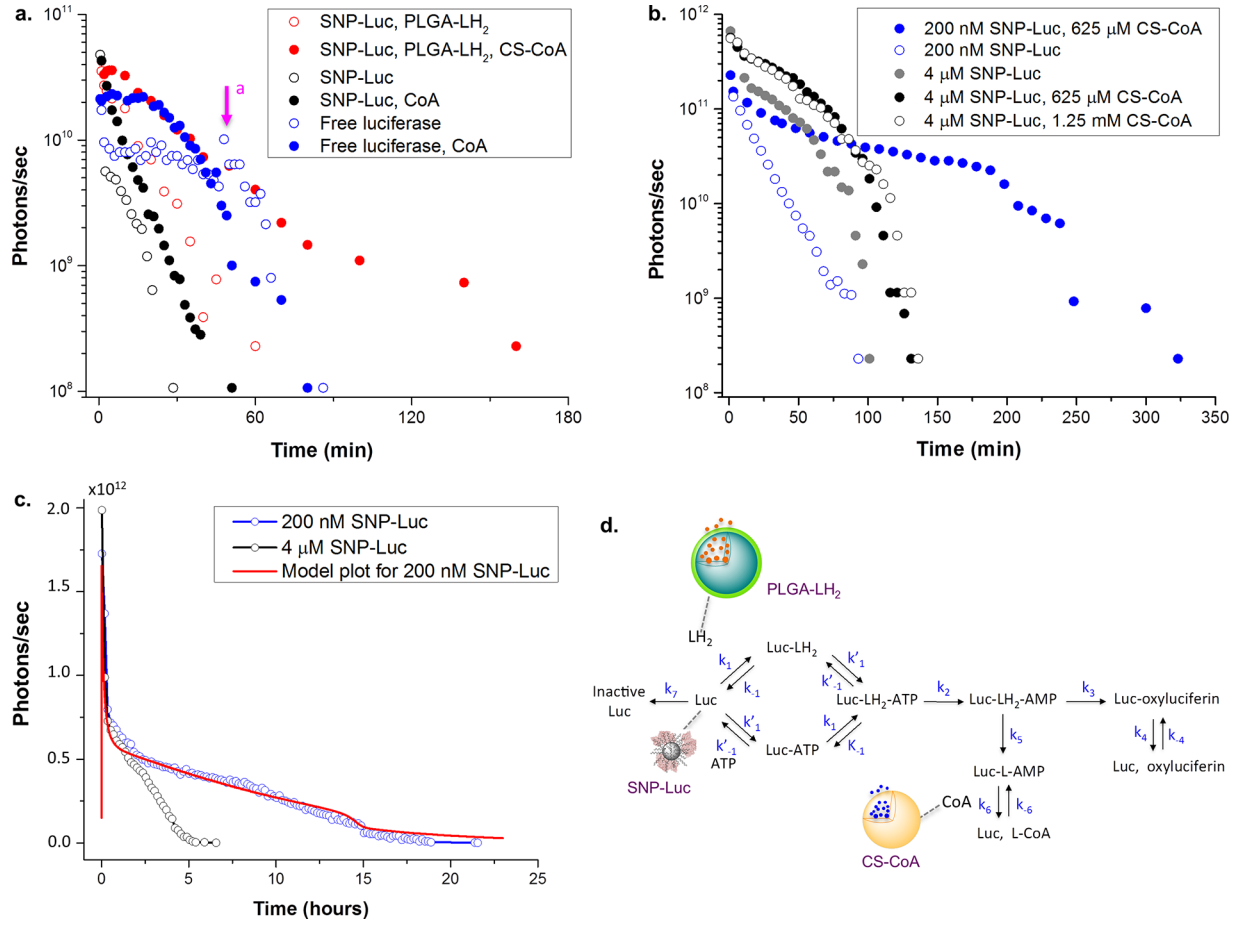


**Figure 2.** Nanoparticle-mediated light production in vitro. (a) Comparison of light production between with and without nanoparticles; evaluation was carried out in a 1 mL mixture containing luciferase (12 nM), luciferin (100 $\mu$M), and ATP (100 $\mu$M) with or without coenzyme A (100 $\mu$M) ($n$ = 2). The pink arrow (a) means addition of CoA in the middle of the reaction. (b) Comparison of light duration between high (4 $\mu$M) and low (0.2 $\mu$M) concentration of SNP-Luc at high concentration of CS-CoA (625 $\mu$M) with limited PLGA-$LH_2$ (100 $\mu$M). (c) Light duration at different concentration of SNP-Luc at a high concentration of PLGA-$LH_2$ (1 mM) and CS-CoA (625 $\mu$M). The model plot (red line), which accounted for the reaction rates and releasing kinetics of nanoparticles, showed great fit with experimental data. The light intensity was analyzed by ImageJ from the photos taken with Nikon D5300 at a set of 5 s exposure, $f$/4.5 and ISO 3200. (d) A kinetic model of firefly luciferase–luciferin reaction in the presence of coenzyme A (CoA). Luc; firefly luciferase, $LH_2$; D-luciferin, ATP; adenosine triphosphate, AMP; adenosine monophosphate, L-AMP; dehydroluciferyl AMP, L-CoA; dehydroluciferyl CoA. The light-generating pathway proceeds at a rate of $k_3$ and the side reaction that is not producing photons (also known as dark reaction) occurs at a rate of $k_5$. Natural denaturation rate of luciferase is $k_7$. Luciferase activity is recovered by thiolytic activity of CoA ($k_6$) and releasing oxyluciferin ($k_4$). The values of each reaction rate are described in Supporting Information.

maximum of $4.5 \times 10^{11}$ photons/sec/mL, while light duration can be extended by 2.5 times at 200 nM SNP-Luc with a max rate of $1.5 \times 10^{11}$ photons/sec/mL. Hence, balancing luciferin release from PLGA-$LH_2$ and consumption via reaction 1 is found to be a key consideration for maximizing light production (Figure 2b). For example, in a reaction mixture containing 1 mM PLGA-$LH_2$ with 200 nM SNP-Luc results in enormous duration of approximately 21.5 h compared with 6 h at 4 $\mu$M of SNP-Luc (Figure 2c). This optimization was accomplished by constructing a new chemical kinetic mathematical model by incorporating reaction 2, the reaction rate of dark reaction ($k_5$) and regeneration of enzyme activity by CoA ($k_6$), as well as accounting for reaction 1, the reaction rate of SNP-Luc and releasing kinetics of PLGA-$LH_2$ and CS-CoA (Figure 2d, Table S2, Figure S6), showing excellent agreement with experimental data (Figure 2c).

To insert the nanoparticle mixture into the whole plant, we developed a method of infusion using stomatal pores within the leaves termed pressurized bath infusion of nanoparticles (PBIN). Here, the entire plant is briefly submerged in a pressured aqueous chamber (Figure 3a). The pressurization rate affects the efficiency of PBIN (Figure 3b). When 0.4 bar/s was applied to a spinach leaf, infiltration was completed within 3 s, however damage to the mesophyll was apparent, including ruptured cell membranes as observed by confocal microscopy (Figure S8). PBIN was successful at 0.04 bar/s applied without membrane damage but was notably incomplete at rates below 0.02 bar/s despite reaching the same saturation pressure of 1.8 bar in all cases.

PBIN is able to simultaneously infiltrate the nanoparticle mixture into wild-type spinach, arugula, and watercress but not kale without modification (Figure S9). Water contact angle measurements on either side of a kale leaf show values of 127.5° on the adaxial side and 148.9° on the abaxial side, which are significantly higher than those of spinach, watercress, and arugula, which range from 85.2° to 109.5° (Figure 3c). A nanofluidic model describes how PBIN works by supplying an external pressure against the internal microchannels within the leaf spongy mesophyll, generating an inward flow through the stomatal pores. The net inward velocity is dictated by the sum



DOI: 10.1021/acs.nanolett.7b04369
Nano Lett. 2017, 17, 7951−7961

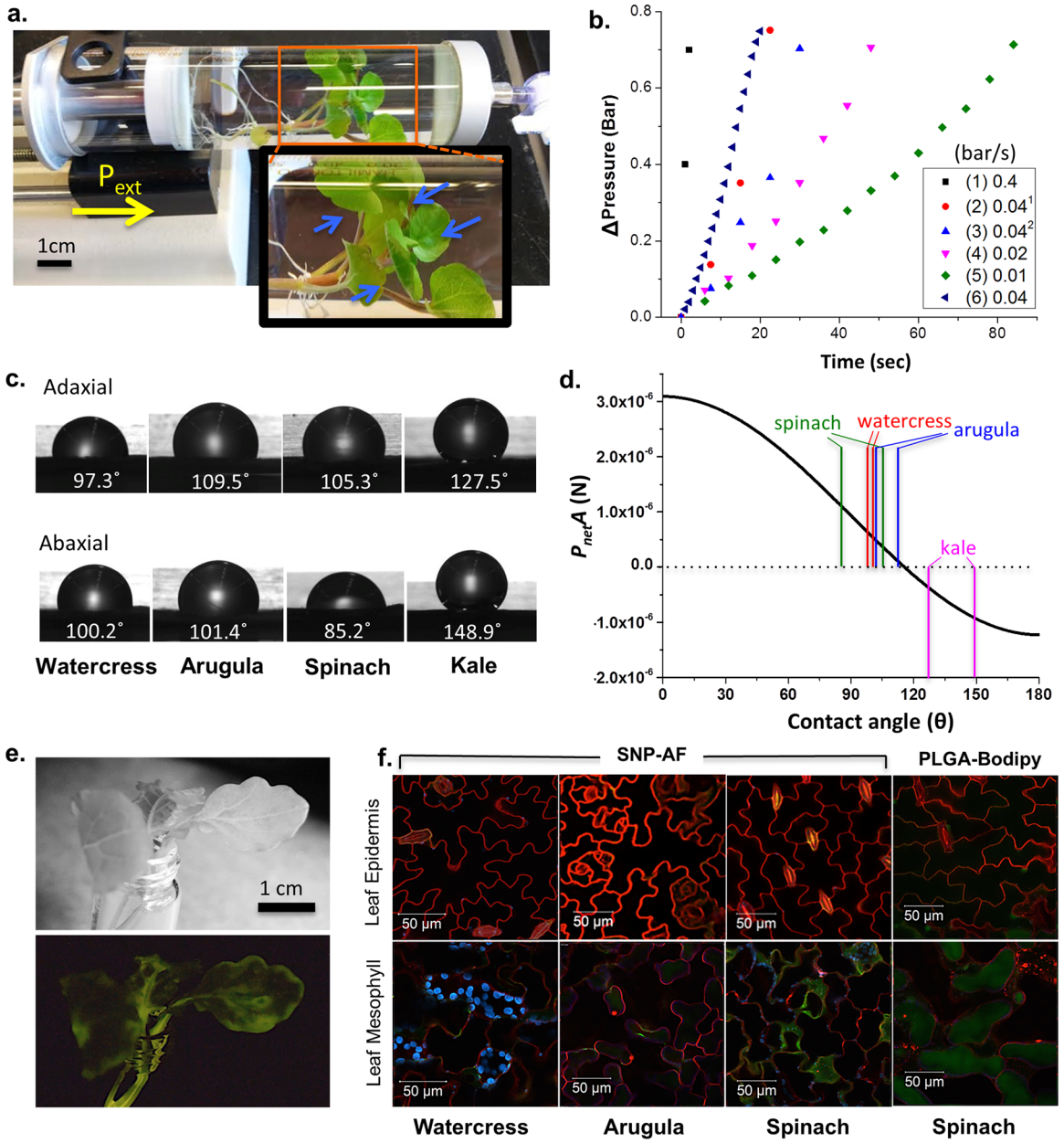


**Figure 3.** Introduction of nanoparticles into living plants. (a) Application of pressurized bath infusion of nanoparticles (PBIN), a whole watercress plant was subjected to PBIN technique. (b) Applied pressure increased at different rates, (1−5) are on a spinach leaf and (6) is a whole watercress plant. Δ Pressure on the *y*-axis the additional pressure with respect to the 1 atm. (c) Contact angle of water drop on the leaves. (d) Correlation between driving force of capillary filling and contact angle of water drop on the leaves, contact angle was measured on the adaxial and abaxial sides of the leaves of watercress, arugula, spinach, and kale. (e) Optical image of 3 week old kale plant (top) and a light-emitting kale after treatment of surfactant (bottom). All the reagents were infiltrated by PBIN. (f) Fluorescent confocal micrographs of dye-labeled silica nanoparticles (SNP-AF, green) and PLGA nanoparticles (PLGA-Bodipy, green) in the leaves of watercress, arugula, and spinach. Red and cyan indicate cell membrane and chloroplast, respectively.

of the capillary forces, viscous drag, resistance from trapped air compression and the applied PBIN force (eq 3)[16]

$$P_{\text{net}}A = 2\sigma w\cos\theta - \frac{12\mu\bar{u}}{h}wx - \frac{hwp_0x}{l-x} + P_{\text{ext}}A \qquad (3)$$

Here, $\sigma$ is the surface tension of water at 25 °C (0.07197 J/m$^2$), $w$ is the diameter of open stomatal pore ($1.5 \times 10^{-7}$ m), and $\theta$ is the contact angle of water drop on the leaf surface (varying) that we measured above. $\mu$ is the dynamic viscosity of water at 25 °C ($10^{-3}$ Ns/m$^2$), $\bar{u}$ is the filling speed determined from PBIN ($4.5 \times 10^{-3}$ m/s), and $h$ is the height of the channel, equal to $w$ at $1.5 \times 10^{-7}$ m. $p_0$ is the initial pressure of the trapped air, that is, atmospheric pressure (101.3 kN/m$^2$), the filling length $x$ ($10^{-2}$ m), and the total length of microchannel $l$ ($1.8 \times 10^{-2}$ m) are estimated from thickness of mesophyll, infiltrated length, and total leaf length. $P_{\text{ext}}$ is the external applied pressure (135 kN/m$^2$), and $A$ is the cross sectional area of the stomatal pore ($1.7 \times 10^{-10}$ m$^2$). Interestingly, eq 3 predicts favorable PBIN infiltration if the plant leaf contact angle is less than approximately 113° (Figure 3d), in close agreement with our observations. We find that the use of a nonionic surfactant *n*-dodecyl-*β*-D-maltoside (0.03 wt %)



DOI: 10.1021/acs.nanolett.7b04369
*Nano Lett.* 2017, 17, 7951−7961

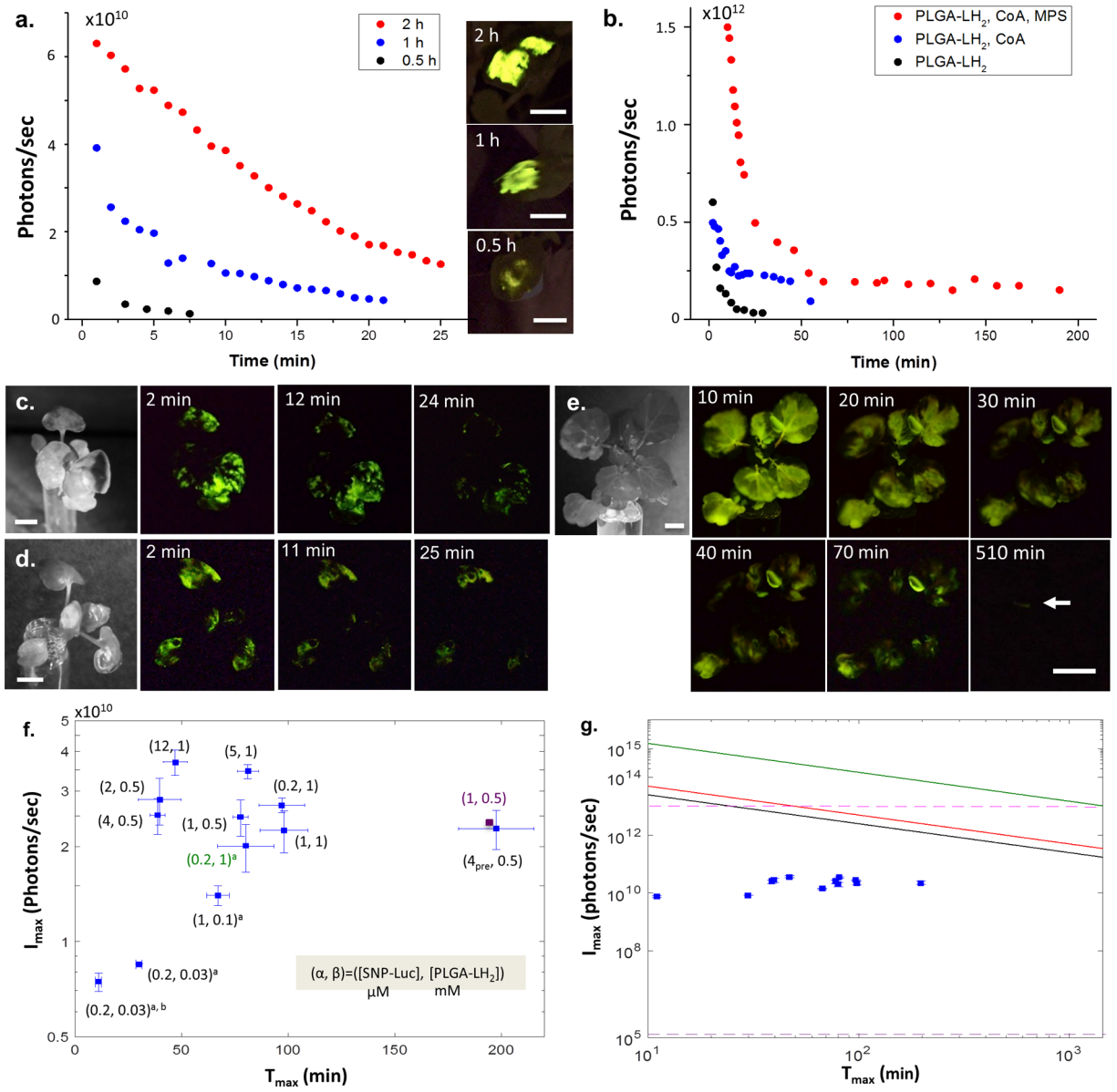


**Figure 4.** Decay kinetics of light emission and its optimization in living plants. (a) Effect of incubation time of SNP-Luc, SNP-Luc (25 $\mu$L, 4 $\mu$M) was infused into the watercress plants by localized infiltration of nanoparticles (LIN) method and the plant was kept in a plant incubator for different time: 30 min, 1 or 2 h. After that, 25 $\mu$L of free luciferin (0.1 mM) was infiltrated. The images on the right panel are obtained from the overlay of the bright-field image and light emission in the dark. (b) Photon number decay of whole glowing plants. PLGA-$LH_2$ (0.1 mM) alone (black dots) or mixture of PLGA-$LH_2$ (0.1 mM) and CS-CoA (50 $\mu$M) (blue dots) was infused into 3 week old watercress plants by PBIN after 1 h of SNP-Luc (4 $\mu$M) infiltration. ATP loaded mesoporous silica nanoparticles (MPS-ATP, 0.2 mg/mL) was preinfiltrated (red dots) to 6 week old watercress plant by PBIN followed by infusion of a mixture of PLGA-$LH_2$ (0.5 mM), CS-CoA (0.625 mM), and SNP-Luc (1 $\mu$M). (c) Time-lapsed photos of a glowing watercress (3 week old) with SNP-Luc and PLGA-$LH_2$, taken by Nikon D5300 with a set of $f$/4.5, ISO 6400, and 30 s to 3.5 min exposure time. (d) Time-lapsed photos of a glowing watercress (3 week old) with SNP-Luc, PLGA-$LH_2$, and CS-CoA, taken by Nikon D5300 with a set of $f$/4.5, ISO 6400, and 1 min exposure time. (e) Time-lapsed photos of glowing watercress (6 week old) with MPS-ATP, SNP-Luc, PLGA-$LH_2$ and CS-CoA, taken by Nikon D5300 with a set of $f$/4.5, ISO 3200, and 30 s exposure except for 70 min (1 min exposure). Scale bars are 1 cm. (f) Summary of maximum photons/sec ($I_{max}$) versus total duration of illumination ($T_{max}$) for different concentration of nanoparticles ($n$ = 3) in a plant tissue ($V$ = 2.5 × $10^{-2}$ $cm^3$). ($\alpha$, $\beta$) = ([SNP-Luc] $\mu$M, [PLGA-$LH_2$] mM), external ATP was supplied by root uptake except for "a" [CS-CoA] = 0.625 mM except for "b" (without CS-CoA), $4_{pre}$ means preincubation of 4 $\mu$M SNP-Luc. Purple square indicates preinfiltration of MPS. The error bars were calculated as a s.d. of at least of triplicate. (g) Comparison of our estimated number of photons/sec from the light-emitting plant (blue squares) to the maximum number of photons/sec calculated at current system (red line, 1 mM PLGA-$LH_2$; black line, 0.5 mM PLGA-$LH_2$). The pink dashed line indicates minimum number of photon/sec for illuminating read text ($10^{13}$ photons/sec), and the green line means the maximum number of photon/sec with 30 mM luciferin to illuminate read text for 1 day. The purple dashed line indicates the maximum photon numbers/sec from a luminescent plant previously reported in ref 3 after accounting the weight of plant tissue (150 mg).

overcomes this unfavorable leaf contact angle (>113°) for PBIN infiltration, resulting in a light-emitting kale plant (Figure 3e). The energy required to pressurize and infuse the plant is the product of the applied PBIN force 5.95 × $10^{-6}$ N and the infusion distance (0.9 × $10^{-2}$ m), or 5.36 × $10^{-8}$ J per stomatal pore. The external applied pressure, $P_{ext}$, of 135 kN/$m^2$ consists



DOI: 10.1021/acs.nanolett.7b04369
Nano Lett. 2017, 17, 7951−7961

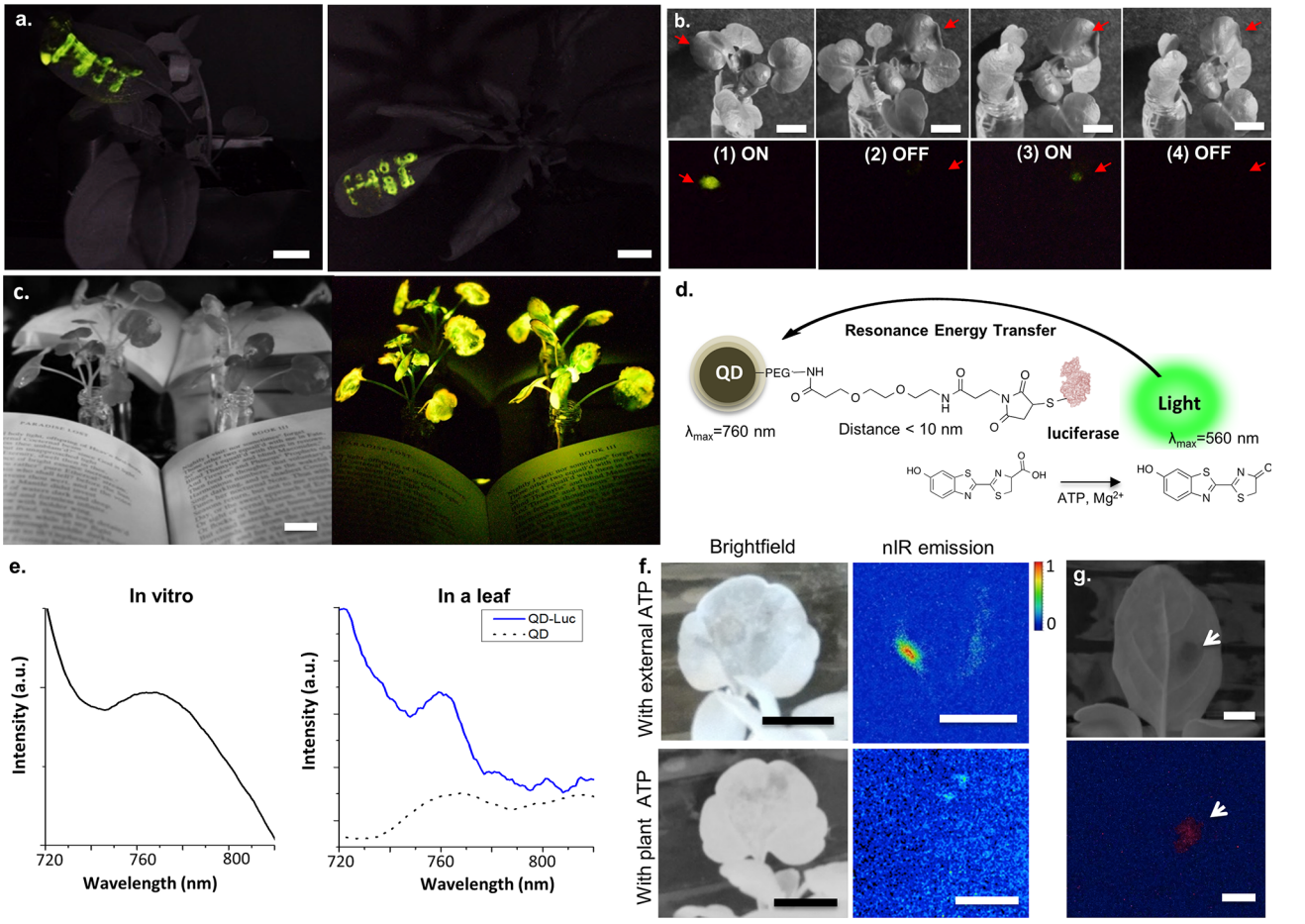


**Figure 5.** Perspective utilization of light-emitting plants. (a) Illuminating MIT logo printed on the leaf of an arugula plant (left) and a spinach plant (right). The mixture of nanoparticles was infused to the leaf by using lab-designed syringe termination adaptors. The images are merged of the bright-field image and light emission in the dark. Photos were taken by Nikon D5300 at a set of 30 s exposure, *f*/4.5 and ISO 6400. Scale bar = 1 cm. (b) Turning on and off of the light-emitting plant. (1) on; with infiltrated mixture of SNP-Luc and PLGA-$LH_2$, (2) off; with an inhibitor of luciferase, dehydroluciferin, (3) on; with CS-CoA to regenerate luciferase activity, and (4) off; with the inhibitor. The bright-field images (top) and glowing spot in the dark (bottom), scale bar = 1 cm. (c) Illumination of a book with light-emitting plants (two 3.5 week old watercress plants). (d) Schematic illustration of shifting the emission wavelength between quantum dots (QDs) and the light production by luciferase−luciferin reaction. (e) Shifted nIR emission spectrum in a cuvette (left) and in a watercress leaf (right) obtained by spectrofluorometer with no laser excitation at 0.1 s integration time. (f) Shifted emission from the living watercress, bright-field (left), and recolored image of nIR emission by ImageJ (right). Strong shifted wavelength emission was detected from the watercress plant with external addition of ATP (top), noticeable nIR emission was observed with plant ATP (bottom). Photos were taken by Raspberry Pi with Night vision camera masked with a 750 nm long-pass filter, 10 s exposure, ISO 800. Scale bar 1 cm. (g) nIR signal as a response to the external chemical, D-luciferin (recolored). QD-Luc was embedded in an arugula plant, and luciferin was added through root uptake.

of 100 kN/m$^2$ due to atmospheric pressure, and the applied 35 kN/m$^2$ gauge pressure.

Uptake and localization of nanoparticles by PBIN is confirmed by using fluorescent confocal microscopy (Figure 3f). Silica nanoparticles labeled with Alexa Fluor 488 (SNP-AF, 7 nm) are observed in every stomata guard cell from all three plant species; spinach, arugula, and watercress, as well as in the leaf mesophyll cells of watercress and arugula, but not spinach. Since the stomata guard cells have an uneven thickness of the cell wall, the stomata open when the guard cells increase in volume, requiring a rapid and massive transport of a solute across the guard cell membrane within minutes.[17,18] This solute transport pathway is consistent with our results that SNP-AF is localized within stomata guard cells. Alternatively, the larger PLGA nanoparticles labeled with BODIPYFL clearly release dye molecules into the intercellular spaces of the mesophyll that, after which the dye will eventually enter the cells.

The rate of decay of the chemiluminescence is found to be strongly dependent on the incubation time of SNP-Luc within the living plants (Figure 4a). Surprisingly, the maximum number of photons/sec is 4.5 times and 7.3 times higher upon 1 and 2 h incubation, respectively, compared to 0.5 h incubation, despite the anticipated loss of luciferase activity with a $t_{1/2}$ of 2 h in live cells.[19] A portion of SNP-Luc localizes within the stomatal guard cells and leaf mesophyll cells but the majority appears to be retained within the substomatal chamber[20] and leaf mesophyll air space in the first 30 min after infiltration. The incubation time is apparently needed to allow for the diffusion of nanoparticles to leave the substomatal chamber, allow penetration of SNP-Luc into the mesophyll and the guard cells, chemically release from PLGA-$LH_2$ or CS-CoA nanoparticles, and finally, the diffusion of the released chemicals across the cell membranes. Hence, we note that control of nanoparticle localization is central to producing bright emission as extracellular ATP concentration is in the micromolar range



DOI: 10.1021/acs.nanolett.7b04369
*Nano Lett.* 2017, 17, 7951−7961

compared with millimolar for the cytosol.[4,21,22] We conclude that the incubation time is an additional key variable to control the localization of SNPs as shown by confocal microscopy images (Figure S10).

As PLGA-$LH_2$ was infused using PBIN to a whole watercress plant grown to maturity for 3 weeks, the initial release of luciferin from PLGA-$LH_2$ nanoparticles resulted in the bright emission of $5.7 \times 10^{11}$ photons/sec (Figure 4b). Despite the sharp drop in intensity after 5 min, light emission continued at 17% of the initial intensity over 30 min (Figure 4b, c). Co-infiltration of CS-CoA extended the duration substantially to more than 1 h with a persistent illumination decreased to 42% of the maximum (Figure 4b,d). Hence, rapid ATP depletion to a diffusion limited rate limits the initial light intensity and the released luciferin flux limits the light duration.

We determine $I_{max}$ is the highest light intensity in photons/sec at the initial measurement and $T_{max}$ is the light duration in minutes evaluated at the camera detection limit of approximately $10^7$ photons/sec. When SNP-Luc is locally infused to a living watercress plant, the maximum intensity appears depressed in lower concentration, while increasing the concentration shortens the duration (Figure 4f). For instance, 200 nM of SNP-Luc shows $I_{max}$ of $2.7 \times 10^{10}$ photons/sec and $T_{max}$ of 97 min, while 12 $\mu$M of SNP-Luc shows $I_{max}$ of $3.7 \times 10^{10}$ photon/sec and $T_{max}$ of 47 min. Since SNP-Luc are the smallest nanoparticles in the mixture, their faster diffusion over the larger PLGA-$LH_2$ and CS-CoA within the leaf mesophyll space allows for their complete distribution if a preincubation step is performed. Preincubation of SNP-Luc results in a beneficial increase to over 3 h of light duration in a living plant (Figure 4f). To circumvent nanoparticle diffusion as a limitation, we find that preinfiltration of mesoporous silica nanoparticles (MPS) to fill the microchannels within the leaf mesophyll acts to slow reactive nanoparticle diffusion, yielding over 3 h of light duration (Figure 4f). It appears to be critical to keep the chemiluminescent reactive zones continuously supplied with reagents. For example, reducing the concentration of PLGA-$LH_2$ from 1 to 0.5 mM shows little change in intensity and duration, but light emission falls considerably below 0.1 mM. Accordingly, the light duration in a living plant is notably extended with preinfiltration of MPS, 1 $\mu$M SNP-Luc, 0.5 mM PLGA-$LH_2$, and 625 $\mu$M CS-CoA (Figure 4b,e) in the bright emission of $1.44 \times 10^{12}$ photons/sec (Figure 4b), or nearly 0.51 $\mu$W as converted to power at 560 nm. We note that this is approximately 50% of an 1 $\mu$W commercial LED. Despite this, the light decay rate remains heterogeneous with one region continuing to emit for 8.5 h (Figure 4e).

The maximum possible photons ($N$) available for emission in the plant, after accounting for tissue reabsorption, is limited by the concentration of the limiting reagent $C_{lim}$ in the firefly luciferase–luciferin reaction

$$N = C_{lim} \times V_{plant} \tag{4}$$

where $V_{plant}$ is the volume of light-emitting region in a plant. From the emission decay curve, after integration, one can find an approximate relationship for $N$ that describes the trade-off between the initial maximum intensity $I_{max}$ and the duration $T_{max}$:

$$N \approx \frac{1}{2} \times T_{max} \times I_{max} \tag{5}$$

In this work, the maximum intensity values ($I_{max}$) given the duration ($T_{max}$) show that we are 100,000 brighter than a genetically engineered *Nicotiana tabacum* plant with 10 times longer duration (ref 3 only presented data for 20 min).[3] The only other light-emitting plant in the literature was reported by *Science* in 1986, and required 24 h to integrate enough light for imaging.[2] The model in eq 5 suggests that in this work, the $I_{max}$ values are 2 orders of magnitude below the predicted maximum (Figure 4g). Higher intensities may be possible by enhancing the permeability of SNP-Luc into the mesophyll cells where ATP concentrations are higher, thus avoiding an ATP limitation. At longer times, increasing the loading of $LH_2$ and CoA within their respective nanoparticles to account for the extended flux can eliminate these limitations. If both are achieved, a light duration of more than 17 days (417 h) at $2 \times 10^{10}$ photons/sec can be achieved. This assumes that SNP-Luc stability does not become a limiting factor. We note that further optimization of the infusion, particle concentration as well as complementary genetic engineering will invariably yield further improvement.

The nanobionic approach has other advantages such as the ability to selectively target specific regions within tissues. We designed a syringe applicator in arbitrary letter shapes "M", "I", and "T" with cone-shaped tapering to minimize the loss of solution during pressurization (Figure S15). An illuminated "MIT" logo was selectively infused into the leaves of two different plant species: arugula and spinach (Figure 5a). As a novel light source, the light-emitting plant can be regulated repeatedly "on" and "off" (Figure 5b) using dehydroluciferin, which is converted to dehydroluciferyl adenylate as an inhibitor, and addition of CS-CoA, which restores the emission back to the "on" state. We benchmarked the luminosity of various plants by comparing the integration time necessary to illuminate a selected text as reference, as shown in Figure 5c for two watercress plants at 300 s exposure with additional ATP or using only the endogenous ATP (Figure S16). To illuminate reading text in real time, we extrapolate this luminosity to a frame rate of 1/12 of a second, yielding the threshold for a comparable sized plant of $10^{13}$ photons/sec. At a sustained release of 30 mM luciferin, our model in eq 5 predicts illumination for 1 day at this threshold for reading text (Figure 4g). At lower fluence, such a light-emitting plant could also be utilized in interior design or indirect, architectural lighting. We also note the utility of local energy generation, storage, and usage of the captured solar fluence, stored ultimately as ATP and consumed locally for lighting, represented by the light-emitting plant.

In addition, it is possible to shift the light emission to other wavelengths using resonant energy transfer to a semiconductor nanocrystal, even to IR wavelengths important for communications. Conjugation of firefly luciferase to a semiconductor nanocrystal or other fluorescent nanoparticle shifts the emission to any alternative wavelength accessible by resonant energy transfer.[23−25] We demonstrate a wavelength shift from the luciferin emission at 560 nm to the near-infrared at 760 nm with 10 nm polyethylene glycol-capped CdSe quantum dots (Figure 5d). The shifted emission at 760 nm was clearly shown in a cuvette containing a mixture of luciferase conjugated quantum dots (QD-Luc), luciferin, and ATP and in a watercress leaf, which were measured by a spectrofluorometer without laser excitation (Figure 5e). When the QD-Luc was infused into living plants, a strong nIR emission signal without external laser excitation was detected using a simple Raspberry Pi CCD camera without IR filter, equivalent to typical smartphone hardware at 6 s exposure. The emission can be



DOI: 10.1021/acs.nanolett.7b04369
*Nano Lett.* 2017, 17, 7951−7961

further enhanced with the addition of ATP, however, nIR emission is clearly detectable using the plant's ATP exclusively (Figure 5f). The QD-Luc system-embedded leaf of an arugula plant visibly shows nIR signal when it detects luciferin via root uptake (Figure 5g). These demonstrations illustrate the potential for ambient IR communications from a plant system, with future work to address control of IR signal modulation and multiplexing for plant-based communications to external electronic devices.

In summary, we show for the first time the use of plants as self-powered light sources using exclusive nanotechnology approaches. We rationally design nanoparticles of controlled size, surface charge and biocompatibility for plant tissue localization to control biochemical pathways in living plants for new functions; converting native ATP to chemiluminescence. This enables entire glowing plants, tissue specific patterning, and wavelength modulation through resonant energy transfer to create wild-type plants with persistent photonic sources for indirect lighting and IR communications. Our technique PBIN is a newly developed method to deliver a mixture of nanoparticles to an entire living plant, and well described by a nanofluidic mathematical model. We also introduce a detailed kinetic model for the description of how chemically interacting nanoparticles interface with existing biochemical pathways in the plant to convert ATP to photons for illumination. We note that the design rules utilized for these nanoparticles also extend to broader applications, including gene delivery, biosynthesis, fertilizer, and pesticides.

**Plant Growth.** All the experiments were carried out on 3−4 weeks old lab-grown plants. Seeds were purchased from David's gardens seeds (TX, U.S.A.) and Renee's Garden (CA, U.S.A.). Spinach (*Spinacia oleracea,* carmel and catalina), arugula (*Eruca sativa*), watercress (*Nasturtium officinale*) and kale (*Brassica oleracea*) were grown in a plant growth chamber (Adaptis 1000, Conviron, Canada) at set condition of 60% humidity, 22 °C/18 °C, medium light intensity, and 16 h light/8 h dark. We counted the plant age from seeding.

**Preparation of Dye-conjugated Silica Nanoparticles (SNP-AF).** Twenty-five microliters of (3-glycidyloxypropyl)-trimethoxysilane (GPTS, Sigma, MO, U.S.A.) was added to 100 $\mu$L of 75% ethanol/water to be hydrolyzed for 1 h at room temperature. GPTS was added to 0.5 mL of silica nanoparticles (10 mg/mL, $1.9 \times 10^{16}$ particles/mL Nanocomposix, CA, U.S.A.) in 2.5 mL of 80% of ethanol/water, then the temperature gradually increased up to 65 °C and the reaction was continued for 24 h. GPTS−silica nanoparticles were washed with ethanol and water multiple times by using centrifugal filter (Mw cutoff 30 kDa, Millipore, MA, U.S.A.) at 1,250 rpm for 15 min. Two hundred micrograms of Alexa Fluor 488-cadaverine (Invitrogen, MA, U.S.A.) was added to 2 mL of GPTS-SNP (1 mg/mL). This reaction was continued for another 24 h at 65 °C. Alexa Fluor 488 conjugated silica nanoparticles (SNP-AF) were washed with water thoroughly until the filtrated solution had no detectable absorbance at 493 nm.

**Preparation of BODIPYFL Encapsulated PLGA Nanoparticles (PLGA-Bodipy).** BODIPYFL (Invitrogen), hydrophobic fluorescent dyes, encapsulated PLGA nanoparticles were prepared by a nanoprecipitation technique.[26,27] One milligram of the dye was dissolved in 0.2 mL of acetone (Sigma), and 10 mg of PLGA (lactide:glycolide 50:50, Mw 30,000−60,000, Sigma) was dissolved in 0.3 mL of acetone. To this mixture, we added 2 mL of 1.5 wt % poly(vinyl alcohol) (PVA, Mw 31,000−50,000, Sigma) aqueous solution with vigorous stirring. The reaction was continued for 2 h followed by evaporation of acetone. The remaining BODIPYFL in the solution was removed by centrifugation multiple times at 8,000 rpm for 10 min.

**Preparation of Luciferase Immobilized Silica Nanoparticles (SNP-Luc).** Ten milliliters of GPTS-silica nanoparticles (10 mg/mL) were reacted with 200 mg of poly(ethylene glycol) bis(amine) ($NH_2$−PEG−$NH_2$, Mw 2,000, Sigma) for 6 h at 65 °C. The excess PEG was removed thoroughly by using a centrifugal filter (Mw cutoff 30 kDa) washing with water multiple times. Maleimide−$PEG_2$−succimidyl ester (MA−$PEG_2$−NHS, Mw 425.39, Aldrich) 4.2 mg was reacted to $NH_2$−PEG anchored silica nanoparticles for 1 h in 10 mM pH 7 phosphate buffer. The resulting MA-PEG-SNP was kept at 4 °C until luciferase immobilization. Firefly luciferase (Promega, MI, U.S.A.) was physically anchored on the PEG chain, which also has electrostatic interaction with positive charge of the amine end groups.[28,29] Also, as luciferase bears cysteine, SH functional group can covalently conjugated to silica nanoparticles via reacting to maleimide group. One milligram of luciferase (12.4 mg/mL) was incubated with 2 mg of SNP-PEG in 30 mM HEPES buffer (pH 7.5) for 1 h at 4 °C with a gentle shaking (600 rpm). Unbound luciferase was gently removed by using a centrifugal filter tube (Mw cutoff 100 kDa) at 4 °C.

**Preparation of Luciferin Encapsulated PLGA Nanoparticles (PLGA-$LH_2$).** D-Luciferin encapsulated PLGA nanoparticles were prepared by the aforementioned nanoprecipitation technique. Five milligram of D-luciferin (Sigma) was dissolved in 1 mL of acetone, and 50 mg of PLGA was dissolved in 1 mL of acetone. These were mixed together, and added to 8 mL of 1.5 wt % poly(vinyl alcohol) (PVA) aqueous solution with vigorous stirring. The reaction was continued for 1 h followed by evaporation of acetone. The remaining luciferin in the solution was removed by centrifugal filter (Mw cutoff 100 kDa). We measured the UV absorbance ($\lambda_{max}$ = 328 nm) of the supernatant after centrifugation, by which we determined the encapsulation yield of luciferin to be 30%.

**Preparation of Coenzyme A Functionalized Chitosan-tripolyphosphate Nanoparticles (CS-CoA).**[30,31] Five milligrams of coenzyme A was mixed with 2 mg/mL of chitosan (medium Mw, Sigma) in 0.3% acetic acid. This mixture was slowly added dropwise to 2 mL of a tripolyphosphate (TPP, Sigma) aqueous solution (1 mg/mL) with magnetic stirring. The reaction was continued for 2−3 h and the remaining coenzyme A was removed by centrifugation at 8,000 rpm for 10 min. As measured the UV absorbance ($\lambda_{max}$ = 258 nm) of supernatant after centrifugation, the encapsulation efficiency of coenzyme A was determined to be 40%.

**Preparation of ATP Loaded Mesoporous Silica Nanoparticles (MPS-ATP).** Amine-functionalized mesoporous silica nanoparticles (200 nm diameter, 4 nm pore size, Aldrich) was incubated with 0.5 mM ATP overnight at 4 °C.

**Preparation of Luciferase Immobilized Quantum Dots (QD-Luc).** Quantum dots functionalized with amine-derivatized PEG ($\lambda_{em}$ = ∼800 nm, 80 $\mu$M, Invitrogen) was conjugated with 1.5 equiv of maleimide−$PEG_2$−succimidyl ester (Aldrich) for 1 h in 10 mM pH 7.0 phosphate buffer. The unbound maleimide−$PEG_2$−succimidyl ester was thoroughly removed by centrifugation (Mw cutoff 50 kDa) multiple times. Luciferase was covalently linked to the maleimide functional group of quantum dots in 10 mM pH 7.0 phosphate buffer for



DOI: 10.1021/acs.nanolett.7b04369
*Nano Lett.* 2017, 17, 7951−7961

2 h at 4 °C. The unbound luciferase was gently removed by centrifugal filter (Mw cutoff 100 kDa).

**Characterizaton of Nanoparticles.** Dynamic light scattering (DLS) and phase analysis light scattering zeta potential analyzer (PALS) were used to characterize nanoparticle surface charge and size distribution (NanoBrook ZetaPALS Potential Analyzer, NY, U.S.A.). The average particle size was determined using DLS (averaged over 10 runs) and the nanoparticle surface charge was determined using PALS zeta potential measurement, averaged over 10 runs. The NanoSight LM10 (NanoSight Ltd., Amesbury, United Kingdom) was used to analyze size of PLGA-$LH_2$ and CS-CoA nanoparticles with a finely focused laser beam that is introduced to the nanoparticle suspension through a glass prism.

**Water Drop Contact Angle Measurement.** Contact angle of water drop on leaf surfaces of both leaf abaxial and adaxial sides were measured (Model 200 with manually tilting base and Drop Image Advanced Software, Ramé-Hart, NJ, U.S.A.). A leaf was separated from a 3−4 weeks old plant and cut into an approximately 1 × 1 cm piece, which was held in place using glass coverslips at each edge of the leaf. At least 2 independent measurements were carried out on both leaf adaxial and abaxial sides of each kind of leaf, and the contact angles were averages over 10 measurements.

**Spectrofluorometer Measurement.** A spectrofluorometer (Fluorolog-3, Horiba Jobin Yvon, Japan) was used to measure luminescence in vitro. The reaction mixture totaled 750 $\mu$L including 30 mM pH 7.5 HEPES-$MgCl_2$ buffer, SNP-Luc, luciferin, ATP, and optional coenzyme A and QD-Luc. The cuvette was placed in the spectrofluorometer, and the light emission was monitored under constant mixing with a magnetic stirrer (CIMARECi, Thermo Fisher Scientific, MA, U.S.A.). Leaf light emission was directly measured by inserting the leaf in a sample holder.

**Fluorescent Confocal Micrographs.** Confocal images were taken in a Zeiss LSM 710 NLO microscope (Germany). HEPES-$MgCl_2$ buffer (30 mM, pH 7.5) alone or 0.15 mg/mL of SNP-AF in buffer was infiltrated into leaves as attached to the living plants by the LIN or PBIN method. The leaf was cut immediately or in 2 h after infiltration, and leaf disc (5 mm in diameter) was prepared. Before submerging the leaf disc in FM 4−64 (*N*-3-triethylammoniumpropyl)-4-(6-(4-(diethylamino) phenyl) hexatrienyl) pyridinium dibromide) solution (Sigma, 10 $\mu$g/mL) to stain cell membranes, 5−10 holes were made in the lower side of the leaf to improve penetration of the dye. After another 2 h, the leaf disc was transferred to a glass slide having a polydimethylsiloxane (PDMS, Carolina Observation Gel, NC, U.S.A.) chamber filled with perfluorodecalin (PFD, Sigma) on the glass slide.[32] The slide was sealed with a coverslip and imaged with a 40× water immersion objective.

**Infiltration of Nanoparticles in Living Plants.** Localized infiltration of nanoparticles (LIN) technique requires nanoparticle suspensions to be infiltrated through the leaf abaxial side of leaf using a 1 mL volume syringe (NORM-JECT, Germany). For pressurized bath infusion of nanoparticles (PBIN), a whole plant is submerged inside a 100 mL volume glass body syringe (Hamilton, NV, U.S.A.) with a luer lock valve containing the nanoparticle suspension followed by pressurization using a syringe pump (KD Scientific Inc. MA, U.S.A.). The pressure was monitored with a digital hydronic manometer (Dwyer instruments, IN, U.S.A.). After infusion of nanoparticles with LIN or PBIN, the infiltrated plants were thoroughly washed with water to remove the remaining nanoparticles on the surfaces. The nanoparticle suspension for PBIN was prepared in 80 mL of 30 mM pH 7.5 HEPES-$MgCl_2$ buffer including the reactive nanoparticles.

**Estimation of Photon Numbers from Light-Emitting Plants.** We first measured the power of an LED light source at $r$ = 12.70 cm away from a photodetector (wavelength $\lambda$ = 530 nm, detector surface area $A$ = 1 $cm^2$) using a PM100D Digital Meter (ThorLabs, NJ, U.S.A.) coupled with a Slim Si (S130C) sensor. The number of photons incident on the photodetector was determined using the measured power ($P'$ = 10 nW) divided by the energy of a single photon at 530 nm, given by the equation below:

$$E_{\text{photon}} = \frac{hc}{\lambda} = \frac{6.63 \times 10^{-34} \times 3 \times 10^{8}}{530 \times 10^{-9}} = 3.75 \times 10^{-19} J$$

where $E_{\text{photon}}$ is the energy of one photon at 530 nm, $h$ is Planck's constant, and $c$ is the speed of light ($3 \times 10^8$ m/s). The total photons/s from the LED light (assuming a point source) is

$$P_{\text{LED}} = \frac{4\pi r^2}{A} P' = 20270 \text{ nW} = 5.47 \times 10^{13} \text{ photons/s}$$

An image of the LED light was taken from a distance of $r_1$ = 68.58 cm at $t_{\text{LED}}$ = 1/1000 s exposure to avoid saturation of pixels. All pixel responses were converted into quantitative values using ImageJ and summed together (Mean value = 0.016). This value corresponds to an incident energy $E_1 = P_{\text{LED}} t_{\text{LED}} \frac{A_1}{4\pi r_1^2} = 1.43 \times 10^5$ photons (with $P_1 = E_1/t_{\text{LED}} = 1.43 \times 10^8$ photons/sec) on the camera aperture ($A_1$ = 0.155 $cm^2$, $f$ = 20 mm). An image of the light-emitting plant was taken with a similar protocol at a distance of $r_2$ = 20 cm with $t_{\text{LED}}$ = 30 s exposure and converted into quantitative values using ImageJ (Mean value = 7.375), corresponding to an incident $E_2 = \frac{7.375}{0.016} E_1 = 6.59 \times 10^7$ photons on the camera aperture ($A_2$ = 0.155 $cm^2$, $f$ = 20 mm). The total energy stemming from the light-emitting plant can hence be estimated as $E_{\text{LEP}} = E_2 \frac{4\pi r_2^2}{A_2} = 2.14 \times 10^{12}$ photons (with $P_{\text{LEP}} = E_{\text{LEP}}/P_{\text{LEP}} = 7.12 \times 10^{10}$ photons/sec), assuming $1/r^2$ intensity dependence.

After accounting for tissue reabsorption, where $\mu$ is the optical density of a nanoparticle infiltrated leaf (104.4 $cm^{-1}$ at 560 nm wavelength, Figure S13), $x$ is the distance from the incident light (125 $\mu$m), the estimated photons of the light-emitting plant is

$$7.12 \times 10^{10} \times e^{\mu x} = 1.44 \times 10^{12} \text{ photons/s}$$

**Estimation of Limiting Reagent for the Approximation of the Maximum Photon Numbers.** Generally, the total emitted number of photons ($N$) depends on the concentration of luciferin, ATP, luciferase and CoA. Assuming 100% conversion efficiency of D-luciferin to oxyluciferin under the excess amount of active luciferase and continuous supply of ATP, $C_{\text{lim}}$ corresponds to the concentration of luciferin, $C_{\text{luciferin}}$. This sets the upper limit for our estimate; for example, 1 mM D-luciferin in the luminescent region of $2.5 \times 10^{-2}$ $cm^3$ ($V$) can emit no more than $1.5 \times 10^{16}$ photons.

**Approximation of the Threshold for Reading Text.** The threshold is determined by the light emission with 4 $\mu$M SNP-Luc, 0.5 mM PLGA-$LH_2$, 0.625 mM CS-CoA, and 0.5 mM ATP, which corresponds to $2.81 \times 10^{10}$ photons/sec



DOI: 10.1021/acs.nanolett.7b04369
*Nano Lett.* 2017, 17, 7951−7961

(Figure 4g). The text (font size 14, bold) can be clearly seen at 30 s exposure with the aforementioned condition (Figure S14). Considering the frame rate of a human eye (12 frames per second), the threshold intensity for reading text can be estimated as $2.81 \times 10^{10} \times 30 \times 12 = 1.01 \times 10^{13}$ (photons/sec)

**Regulation of Turn on/off the Light Emission in a Living Plant.** SNP-Luc (0.5 mg/mL, 4 $\mu$M of luciferase, 25 $\mu$L) was infiltrated by LIN and followed by infiltration of PLGA-$LH_2$ to turn on the light. Dehydroluciferin (6 $\mu$M, 25 $\mu$L) was added to turn off, and then coenzyme A (27 $\mu$M, 25 $\mu$L) was infiltrated to regenerate luciferase activity, which turns on the light again. The light emission could be diminished naturally as consuming ATP and luciferin, or turned off immediately by infiltration of dehydroluciferin.

**Illumination of a Book.** SNP-Luc (4 $\mu$M of luciferase, 100 $\mu$L for each leaf) was infiltrated by LIN in two watercress plants (3 week old). ATP (1 mM) was added to the plants, followed by infiltration of PLGA-$LH_2$ (0.1 mM) by PBIN. The book "Paradise Lost" and the light-emitting watercress plants were placed in front of a reflective paper to increase the influence from the light-emitting plants to the book pages. The photo was taken with a Nikon D5300 set at 5 min exposure, $f$/4.5, and ISO 3200.

**Fabrication of Syringe Applicator.** The syringe applicators were designed in AutoCad, and fabricated by using a LulzBot Mini Desktop 3D printer (Aleph Objects, Inc. CO, U.S.A.) with plastic filament (High impact polystyrene; HIPS, 3 mm).

**Detection of nIR Emission with Raspberry Pi.** A Raspberry Pi equipped with a $f$ = 3.6 mm 1/2.7″ camera with IR filters removed (SainSmart Infrared Night Vision Surveillance Camera, KS, U.S.A.) was used. To detect nIR emission from the QD-Luc embedded within the living plant, a FEL0750 long pass filter (ThorLabs Inc.) was placed in front of the camera lens, and images were collected at 6 s exposure with an ISO 800. The mixture comprised of 100 $\mu$L 30 mM pH 7.5 HEPES-$MgCl_2$ buffer containing QD-Luc or SNP-Luc, 100 $\mu$M free luciferin, and with or without 100 $\mu$M ATP, was infiltrated into the watercress plant. The roots of a QD-Luc embedded-arugula plant were submerged in 20 mL of luciferin solution (1 mM) with 1 mM ATP in 30 mM HEPES buffer. In 10 min under the light, nIR emission masked with the 750 nm long pass filter was detected. The image was collected at 6 s exposure with ISO 800.

## ■ ASSOCIATED CONTENT

### Supporting Information

The Supporting Information is available free of charge on the ACS Publications website at DOI: 10.1021/acs.nanolett.7b04369.

FT-IR spectroscopy, analysis of the size distribution of nanoparticles, a kinetic model for luciferase−luciferin reaction containing nanoparticles in vitro, fluorescence confocal micrographs of spinach leaves infiltrated dye-labeled nanoparticles, fluorescence confocal micrographs of spinach leaves infiltrated by PBIN, PBIN method applied to a kale plant, fluorescent confocal micrographs of spinach leaves at different incubation times of nanoparticles, effect of incubation time of nanoparticle on luminescence in living plant, diffusion in a living plant, absorbance of a watercress leaf after infiltration of nanoparticles, illumination of reading text with a different exposure time, a design a syringe applicator, light-emitting plant as a desk lamp powered by ATP generation from photosynthesis, masked light emission with a long pass filter (PDF)

## ■ AUTHOR INFORMATION


### Corresponding Author

*E-mail: strano@mit.edu. Phone: 617-253-4569.

### ORCID

Juan Pablo Giraldo: 0000-0002-8400-8944
Markita P. Landry: 0000-0002-5832-8522
William A. Tisdale: 0000-0002-6615-5342
Michael S. Strano: 0000-0003-2944-808X


### Author Contributions

S.K. and M.S.S. conceived the experiments and wrote the paper. M.S.S designed the PBIN experiments and the associated mathematical model. S.K., J.P.G., and M.W. performed the experiments and data analysis. V.B.K assisted in the kinetic model. T.T.S.L, J.E., M.C.W., and R.M.S. assisted in the experiments and analysis. M.P.L assisted in the analysis of decay kinetics of photons. W.A.T. and M. W. assisted with the energy transfer concept.

### Notes

The authors declare no competing financial interest.

## ■ ACKNOWLEDGMENTS

The authors acknowledge funding from the U.S. Department of Energy under contract 0000215305 to M.S.S. V.B.K. is supported by The Swiss National Science Foundation (Project No. P2ELP3_162149). The authors are grateful for useful discussions with N. Melosh, R. Hurt, E. Biddinger, J. Collins, and S. Kennedy.

## ■ REFERENCES


(1) Giraldo, J. P.; Landry, M. P.; Faltermeier, S. M.; McNicholas, T. P.; Iverson, N. M.; Boghossian, A. A.; Reuel, N. F.; Hilmer, A. J.; Sen, F.; Brew, J. A.; Strano, M. S. *Nat. Mater.* **2014**, *13*, 400−408.

(2) Ow, D. W.; De Wet, J. R.; Helinski, D. R.; Howell, S. H.; Wood, K. V.; DeLuca, M. *Science* **1986**, *234*, 856−859.

(3) Krichevsky, A.; Meyers, B.; Vainstein, A.; Maliga, P.; Citovsky, V. *PLoS One* **2010**, *5*, e15461.

(4) Kim, S.-Y.; Sivaguru, M.; Stacey, G. *Plant Physiol.* **2006**, *142*, 984−992.

(5) Boghossian, A. A.; Sen, F.; Gibbons, B. M.; Sen, S.; Faltermeier, S. M.; Giraldo, J. P.; Zhang, C. T.; Zhang, J.; Heller, D. A.; Strano, M. S. *Adv. Energy Mater.* **2013**, *3*, 881−893.

(6) Wong, M. H.; Misra, R. P.; Giraldo, J. P.; Kwak, S.-Y.; Son, Y.; Landry, M. P.; Swan, J. W.; Blankschtein, D.; Strano, M. S. *Nano Lett.* **2016**, *16*, 1161−1172.

(7) Wong, M. H.; Giraldo, J. P.; Kwak, S.-Y.; Koman, V. B.; Sinclair, R.; Lew, T. T. S.; Bisker, G.; Liu, P.; Strano, M. S. *Nat. Mater.* **2016**, *16*, 264−272.

(8) DeLuca, M. *Adv. Enzymol. Relat. Areas Mol. Biol.* **2006**, *44*, 37−68.

(9) Nakatsu, T.; Ichiyama, S.; Hiratake, J.; Saldanha, A.; Kobashi, N.; Sakata, K.; Kato, H. *Nature* **2006**, *440*, 372−376.

(10) Seliger, H. H.; McElroy, W. D. *Arch. Biochem. Biophys.* **1960**, *88*, 136−141.

(11) Mateo, C.; Palomo, J. M.; Fernandez-Lorente, G.; Guisan, J. M.; Fernandez-Lafuente, R. *Enzyme Microb. Technol.* **2007**, *40*, 1451−1463.

(12) Fraga, H.; Fernandes, D.; Fontes, R.; Esteves da Silva, J. C. G. *FEBS J.* **2005**, *272*, 5206−5216.




DOI: 10.1021/acs.nanolett.7b04369
*Nano Lett.* 2017, 17, 7951−7961

(13) Marques, S. M.; Esteves da Silva, J. C. G. *IUBMB Life* **2009**, *61*, 6−17.
(14) Eichert, T.; Kurtz, A.; Steiner, U.; Goldbach, H. E. *Physiol. Plant.* **2008**, *134*, 151−160.
(15) Hoefnagel, M. H. N.; Atkin, O. K.; Wiskich, J. T. *Biochim. Biophys. Acta, Bioenerg.* **1998**, *1366*, 235−255.
(16) Phan, V. N.; Yang, C.; Nguyen, N.-T. Capillary Filling in Nanochannels. Proceedings of *ASME 2009 7th International Conference on Nanochannels, Microchannels, and Minichannels*; Pohang, South Korea, June 22−24, 2009ASME: pp 907−915. DOI: 10.1115/ICNMM2009-82049.
(17) Atwell, B. J.; Kriedemann, P. E.; Turnbull, C. G. N. *Plants in Action*; Macmillan Education, 1999.
(18) Schroeder, J. I.; Raschke, K.; Neher, E. *Proc. Natl. Acad. Sci. U. S. A.* **1987**, *84*, 4108−4112.
(19) Ignowski, J. M.; Schaffer, D. V. *Biotechnol. Bioeng.* **2004**, *86*, 827−834.
(20) Roth-Nebelsick, A. *Ann. Bot.* **2007**, *100*, 23−32.
(21) Song, C. J.; Steinebrunner, I.; Wang, X.; Stout, S. C.; Roux, S. J. *Plant Physiol.* **2006**, *140*, 1222−1232.
(22) Blatt, M. R. *Planta* **1987**, *170*, 272−287.
(23) Alam, R.; Karam, L. M.; Doane, T. L.; Zylstra, J.; Fontaine, D. M.; Branchini, B. R.; Maye, M. M. *Nanotechnology* **2014**, *25*, 495606.
(24) Frangioni, J. V. *Nat. Biotechnol.* **2006**, *24*, 326−328.
(25) So, M.-K.; Xu, C.; Loening, A. M.; Gambhir, S. S.; Rao, J. *Nat. Biotechnol.* **2006**, *24*, 339−343.
(26) Murakami, H.; Kobayashi, M.; Takeuchi, H.; Kawashima, Y. *Int. J. Pharm.* **1999**, *187*, 143−152.
(27) Makadia, H. K.; Siegel, S. J. *Polymers* **2011**, *3*, 1377−1397.
(28) Hong, R.; Fischer, N. O.; Verma, A.; Goodman, C. M.; Emrick, T.; Rotello, V. M. *J. Am. Chem. Soc.* **2004**, *126*, 739−743.
(29) Sun, X.; Zhao, Y.; Lin, V. S. Y.; Slowing, I. I.; Trewyn, B. G. *J. Am. Chem. Soc.* **2011**, *133*, 18554−18557.
(30) Venkatesan, C.; Vimal, S.; Hameed, A. S. S. *J. Biochem. Mol. Toxicol.* **2013**, *27*, 406−411.
(31) Ribeiro, Â. R.; Santos, R. M.; Rosário, L. M.; Gil, M. H. *J. Biolumin. Chemilumin.* **1998**, *13*, 371−378.
(32) Littlejohn, G. R.; Love, J. *J. Visualized Exp.* **2012**, No. 59, 3394.



DOI: 10.1021/acs.nanolett.7b04369
*Nano Lett.* 2017, 17, 7951−7961